Taylor & Francis
Taylor & Francis Group

Synthetic Communications

An International Journal for Rapid Communication of Synthetic Organic Chemistry

ISSN: (Print) (Online) Journal homepage: https://www.tandfonline.com/loi/lsyc20

Synthesis, characterization, computational chemical studies and antiproliferative activity of some heterocyclic systems derived from 3-(3-(1,3-diphenyl-1*H*-pyrazol-4-yl)acryloyl)-2*H*-chromen-2-one

Mohamed M Kaddah, Abdelgawad A. Fahmi, Mustafa M. Kamel, Sayed K. Ramadan & Sameh A. Rizk

To cite this article: Mohamed M Kaddah, Abdelgawad A. Fahmi, Mustafa M. Kamel, Sayed K. Ramadan & Sameh A. Rizk (2021): Synthesis, characterization, computational chemical studies and antiproliferative activity of some heterocyclic systems derived from 3-(3-(1,3-diphenyl-1*H*-pyrazol-4-yl)acryloyl)-2*H*-chromen-2-one, Synthetic Communications, DOI: 10.1080/00397911.2021.1904991

To link to this article: https://doi.org/10.1080/00397911.2021.1904991

SYNTHETIC COMMUNICATIONS®
https://doi.org/10.1080/00397911.2021.1904991

Taylor & Francis
Taylor & Francis Group

Synthesis, characterization, computational chemical studies and antiproliferative activity of some heterocyclic systems derived from 3-(3-(1,3-diphenyl-1*H*-pyrazol-4-yl)acryloyl)-2*H*-chromen-2-one

Mohamed M Kaddah[a], Abdelgawad A. Fahmi[b], Mustafa M. Kamel[c], Sayed K. Ramadan[a], and Sameh A. Rizk[a]

[a]Department of Chemistry, Faculty of Science, Ain Shams University, Cairo, Egypt; [b]Department of Chemistry, Faculty of Science, Cairo University, Giza, Egypt; [c]Industrial Area, El-Nasr Company for Intermediate Chemicals, Giza, Egypt

ABSTRACT

The key material, 3-(3-(1,3-diphenyl-1*H*-pyrazol-4-yl)acryloyl)-2*H*-chromen-2-one **(3)** was synthesized and its behavior toward malononitrile, hydrazine, thiourea, thiosemicarbazide, 2-aminoaniline, and 6-aminothiouracil was investigated aiming to synthesize a new series of pyrazole-based heterocycles, namely, pyranochromene, diazepine, pyrimidochromene, triazepine, benzodiazepine, pyrimidine, and pyrimidopyrimidine derivatives. Density functional theory based on quantum chemical computation outline the structure optimization of the intermediate that reacted to afford the desired product. The antiproliferative screening against HePG-2 and MCF-7 cancer cell lines disclosed that the most potent compounds against two cell lines were **9** and **17** as compared to doxorubicin which may be due to their presence in more tautomeric structures. Also, the minimized energy, dipole moment, ionization potential, transferred electrons, and charge density distribution revealed that the greater value of 0.126 and 0.8 for pyrazole derivatives **9** and **17**, respectively, indicates the maximum transfer of electron and hence, greater tendency of scavenging radicals and rapidly reduce oxygen to superoxide.

GRAPHICAL ABSTRACT

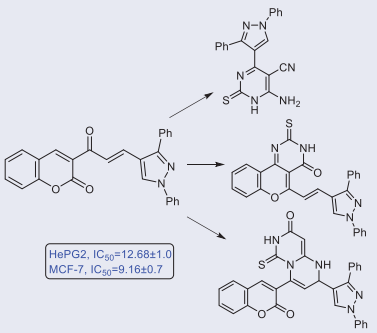

ARTICLE HISTORY
Received 16 January 2021

KEYWORDS
Chromene; pyrazole; pyrimidopyrimidine; triazepine; pyrimidochromene

CONTACT Sayed K. Ramadan sayed.karam2008@sci.asu.edu.eg Department of Chemistry, Faculty of Science, Ain Shams University, Cairo 11566, Egypt.

Supplemental data for this article can be accessed on the publisher's website.

Introduction

Chalcones (1,3-diaryl-2-propane-1-ones) are one of the major classes of natural products with widespread distribution in fruits, vegetables, spices, tea, and soya-based food stuff.[1] Also, chalcones are secondary metabolites obtained from the main precursors of flavonoids and isoflavonoids biosynthesis occurred in terrestrial plants. Otherwise, coumarins and pyrazoles are of great importance due to their pharmacological effects[2–15] (cf. Figure 1). Pyrazoles display anticancer efficacy because of their inhibition of various targets like EGFR, B-raf, ROS1, JAK2, ALK, HDAC, among others.[8–10] Coumarins (benzopyrones) are naturally occurring compounds serving as an important model for design and synthesis of some potent analogues like anticancer, antioxidant, anti-inflammatory, anticoagulation, and estrogenic activities. In many plants, naturally occurring coumarins are found, especially in higher concentrations in tonka bean, woodruff, lavender, licorice, strawberries, apricots, cherries, cinnamon, bison grass and sweet clover. The ability of synthetic coumarin-containing compounds to evoke a wide range of pharmacological effects with a focus on their utility as anticancer therapeutic agents has been shown as its unique skeleton has a special ability to readily interact with a diverse enzymes and receptors in organisms *via* weak bond interactions and therefore a wide potentiality as medicinal drugs.[5,6] In turn, it is well known that chalcones are highly reactive due to α,β-unsaturated carbonyl functionality, which was a good synthon for the synthesis of a variety of heterocyclic systems like pyrazoline, isooxazoline, pyran, pyridine, and pyrimidine derivatives.[16,17] Thus, as an extension of our study,[18–26] we report herein utilization of the chalcone **3** bearing both coumarin and pyrazole scaffolds for the synthesis of some pyrazole-based heterocycles of enhanced antitumor efficacy against two human cancer cell lines, namely, hepatocellular carcinoma (liver) HePG-2 and mammary gland breast MCF-7 cancer cell lines.

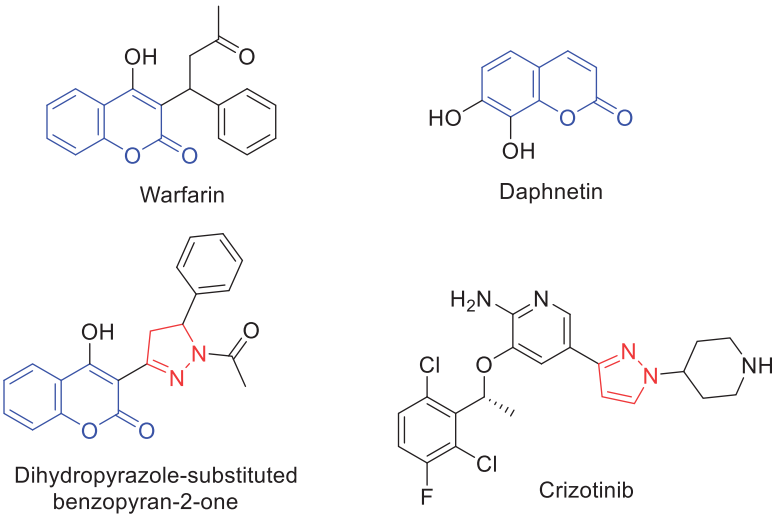

Figure 1. Anticancer, coumarin and pyrazole derivatives.

Results and discussion

Chemistry

Claisen-Schmidt condensation of 3-acetylcoumarin **1** with pyrazole aldehyde **2** [27] achieved the chalcone derivative **3** as yellow crystals (Scheme 1). The IR spectrum displayed coumarinyl C=O at ν 1722 cm^{-1} and ketonic C=O at ν 1655 cm^{-1}. Its ^{1}H NMR spectrum disclosed C5-H of pyrazole at δ 9.29 ppm, C4-H of coumarin at δ 8.65 ppm as well as the aromatic and olefinic protons. Further support for the assigned structure **3** was acquired from its mass spectrum which showed the correct molecular ion peak at *m/z* 418 (22%) and the base peak at *m/z* 77 (100%) corresponding to phenyl cation, in addition to some important fragments (cf. Experimental). Treating chalcone **3** with malononitrile in boiling ethanol and piperidine failed to produce 2-amino-3-cyanopyran derivative **4** and afforded the arylidene malononitrile **5** as a sole product which was identical in all respects with an authentic sample prepared from condensation of pyrazole aldehyde **2** with malononitrile at an ambient temperature (Scheme 1).[28] The reaction pathway can be visualized *via* two routes as displayed in Scheme 2. Noteworthy, the pyranochromene derivative **6** was obtained upon cyclocondensation of **5** with 4-hydroxycoumarin in boiling ethanol and triethylamine. The ^{1}H NMR spectrum of **6** revealed an exchangeable singlet signal for NH_2 and singlet for methine proton in

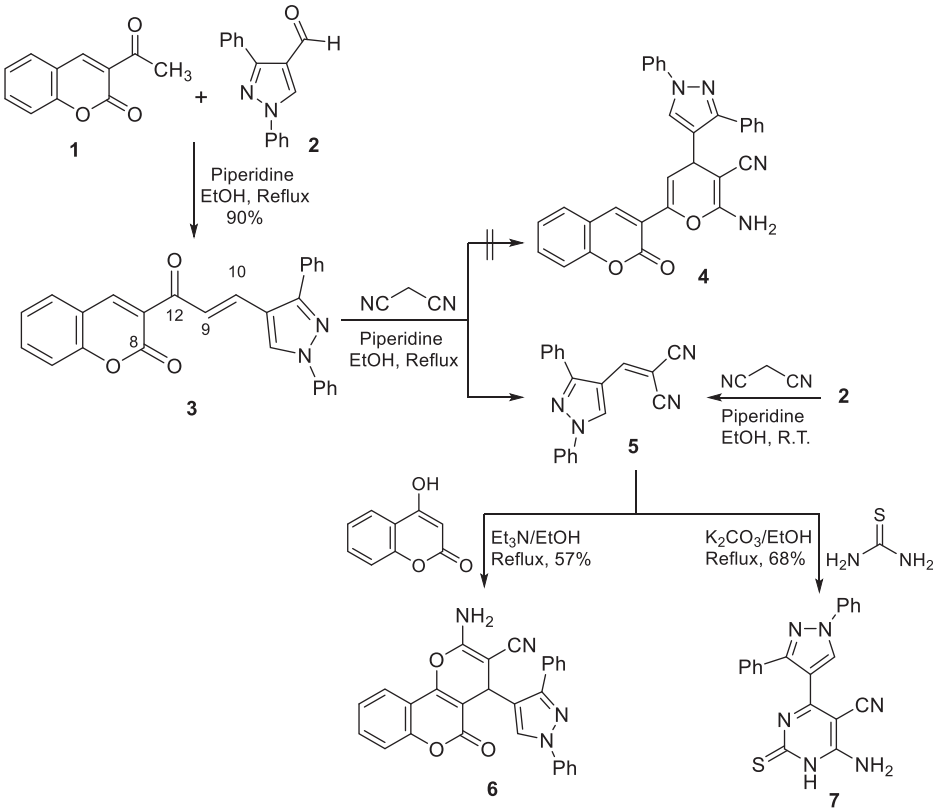

Scheme 1. Synthesis of Chalcone **3** and compounds **5–7**.

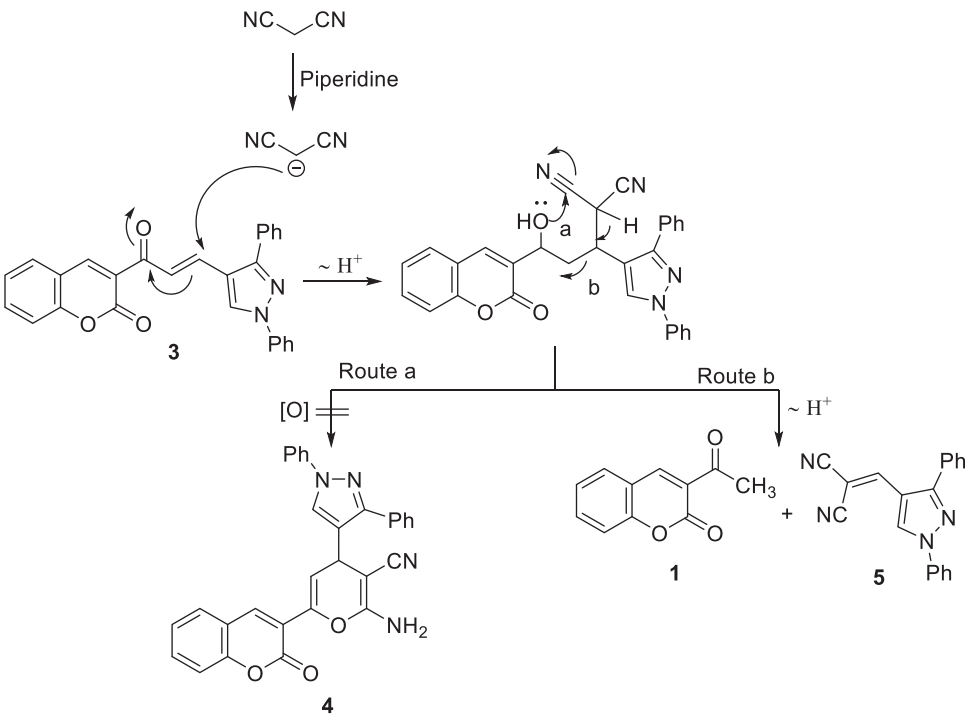

Scheme 2. Plausible pathways for the reaction of chalcone **3** with malononitrile.

addition to the aromatic protons (cf. section "Experimental"). In turn, cyclocondensation reaction of **5** with thiourea in boiling ethanol including anhydrous potassium carbonate led to the formation of 6-aminopyrimidin-5-carbonitrile derivative **7**. Its IR spectrum disclosed bands characteristic for NH, NH_2, C≡N, and C=N groups.

In turn, when chalcone **3** was treated with hydrazine in boiling dioxane, chromenodiazepine derivative **9** was obtained instead of 3-coumarinyl-5-pyrazolylpyrazole derivative **8**. The IR spectrum of **9** revealed the carbonyl functionalities at ν 1722 and 1676 cm^{-1}. In contrast, hydrazinolysis of chalcone **3** in glacial acetic acid afforded the diazepinedione derivative **10** (Scheme 3). The chemical structures were substantiated from their analytical and spectral properties (cf. section "Experimental"). The plausible pathways of hydrazinolysis reaction can proceed *via* two routes as depicted in Scheme 4.

The reaction of chalcone **3** with thiourea was not successful in boiling dioxane while in boiling sodium ethoxide acquired the chromenopyrimidine derivative **12** instead of pyrimidinethione derivative **11** (Scheme 5). The IR spectrum was devoid of C=O of coumarin moiety and displayed ν C=O of amide at 1689 cm^{-1}. The reaction pathway can be extrapolated *via* Scheme 6.

Interaction of chalcone **3** with thiosemicarbazide in boiling dioxane failed to furnish the pyrazole derivative **13** and afforded the triazepinethione derivative **14** (Scheme 7). Its IR and ^{1}H NMR spectra were devoid of NH_2 bands. Further, the highest recorded peak in its mass spectrum was at *m/z* 489 (5%) corresponding to the correct molecular ion peak and the base peak at *m/z* 77 (100%) which is attributable to phenyl cation. In

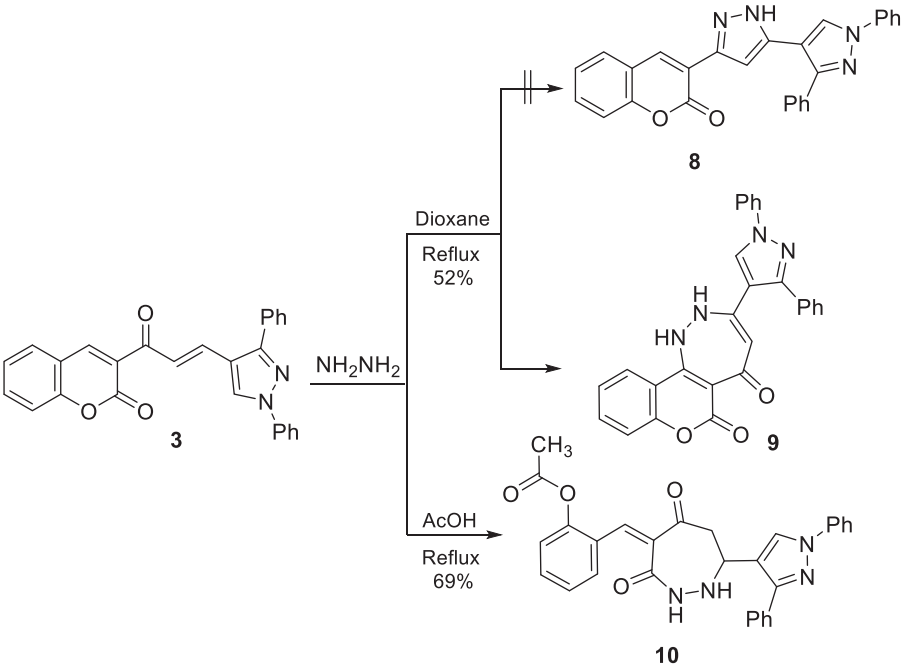

Scheme 3. Reactions of chalcone **3** with hydrazine.

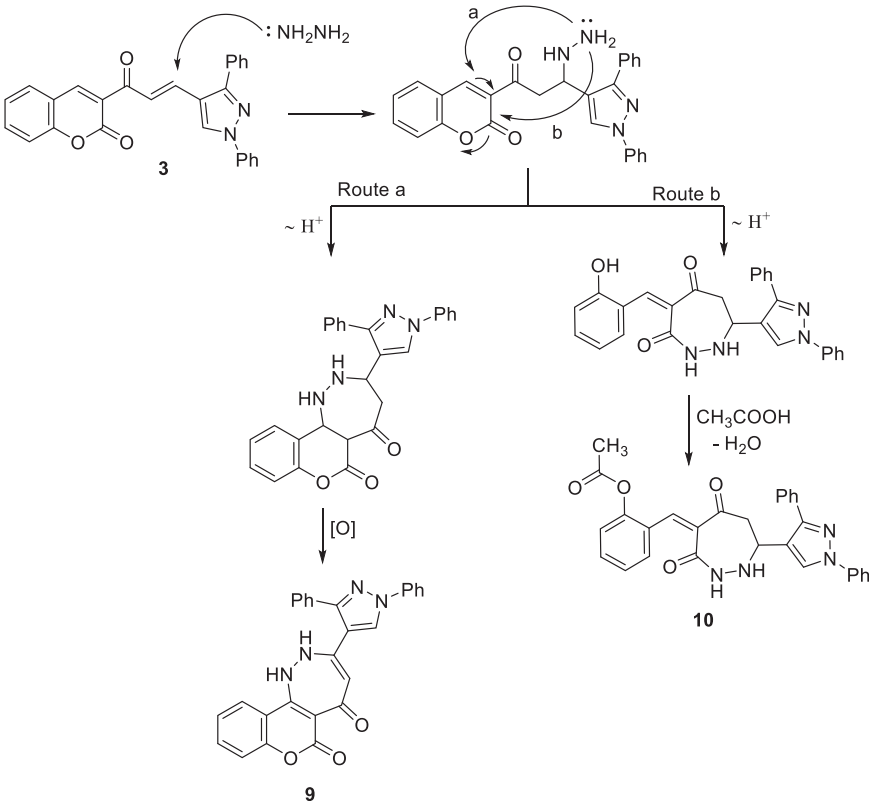

Scheme 4. Plausible pathways for formation of compounds **9** and **10**.

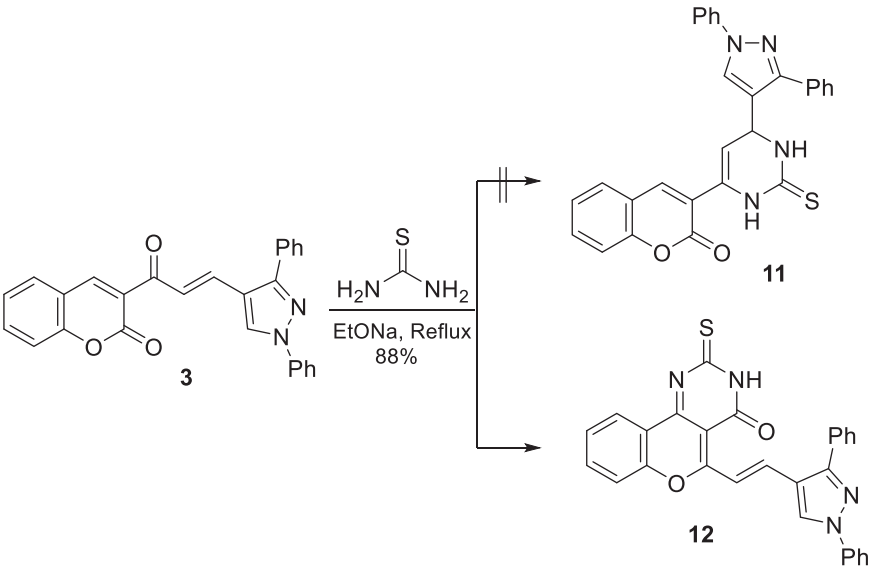

Scheme 5. Reactions of Chalcone **3** with thiourea.

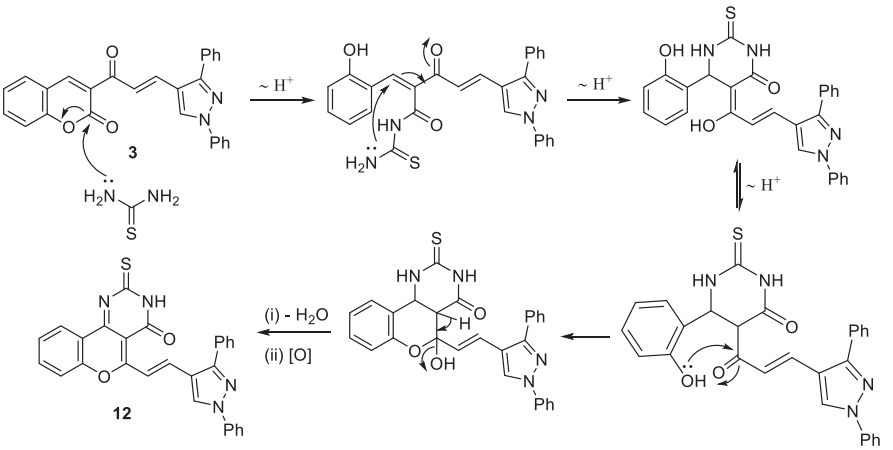

Scheme 6. A suggested pathway for compound **12**.

a similar manner, 2-aminoaniline reacted with chalcone **3** in boiling dioxane to provide benzodiazepine derivative **15**. In contrast, pyridopyrimidine derivative **17** was obtained instead of pyridopyrimidine derivative **16** upon treating chalcone **3** with 6-aminothiouracil in boiling dioxane including piperidine (Scheme 7). The IR spectra conserved the coumarin carbonyl functionality. The reactions can proceed *via* aza-Michael addition followed by ring closure by loss of water.

Density functional theory study

It is well known that high E_{HOMO} are likely to indicate a strong tendency of the molecule to donate electrons. The low values of the energy gap ($\Delta E = E_{LUMO} - E_{HOMO}$)

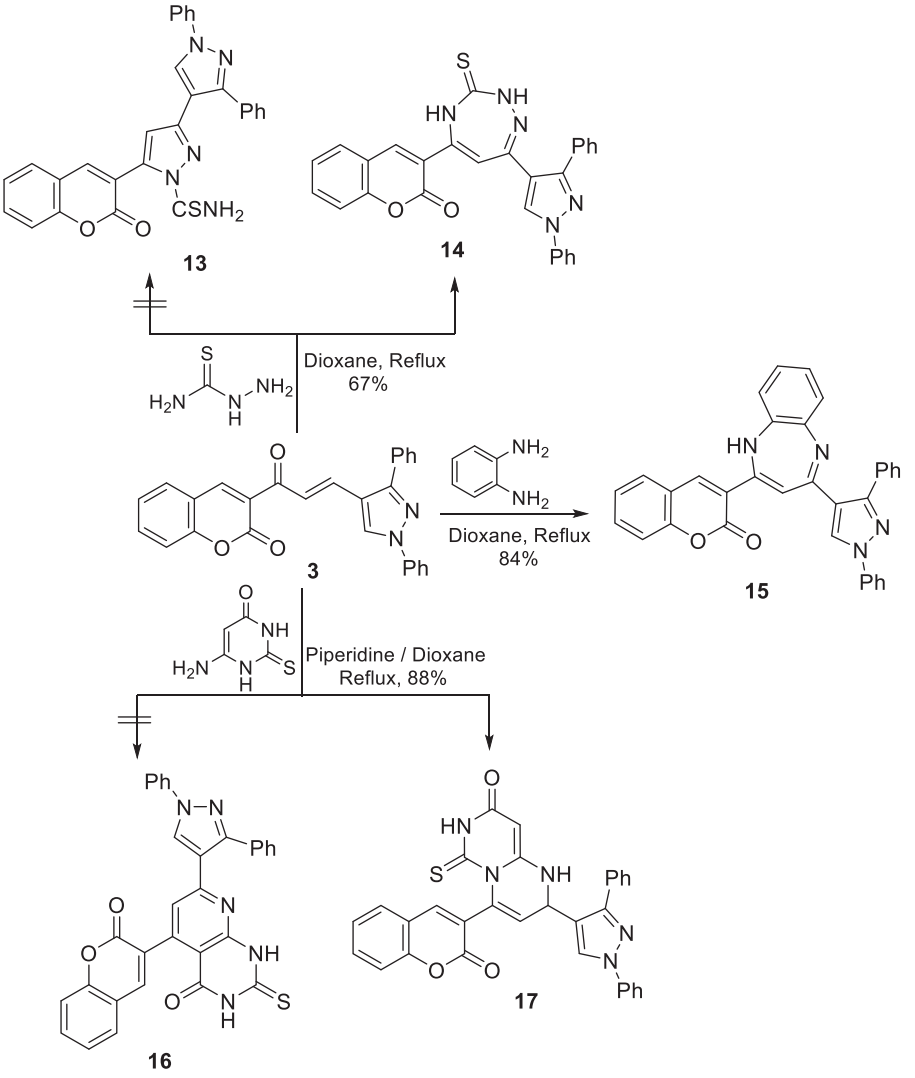

Scheme 7. Reactions of Chalcone **3** with thiosemicarbazide, 2-aminoaniline, and 6-aminothiouracil.

will render good inhibition efficiencies because the energy needed to remove an electron from the last occupied orbital will be low.[29] Density functional theory (DFT) based on quantum chemical computation outline the structure optimization of the intermediate that reacted to afford the desired product. In the presence of reaction of the coumarin chalcone with carbon nucleophile e.g., malononitrile, the HOMO energy (−14.54 eV) rather than HOMO of nitrogen nucleophiles e.g., hydrazine hydrate (−10.83 eV), thiourea (−8.96 eV) and 6-aminothiouracil (−9.05 eV) and so good matching to LUMO energy (−6.37 eV) of the carbonyl electrophilic site of chalcone to form the corresponding new heterocyclic *via* addition reaction followed by cyclization. In the case of using thiosemicarbazide (HOMO −5.32 eV) is more preferred than the HOMO of *o*-phenylenediamine (−7.72 eV) proceeding *via* mechanism of Scheme 7 to form

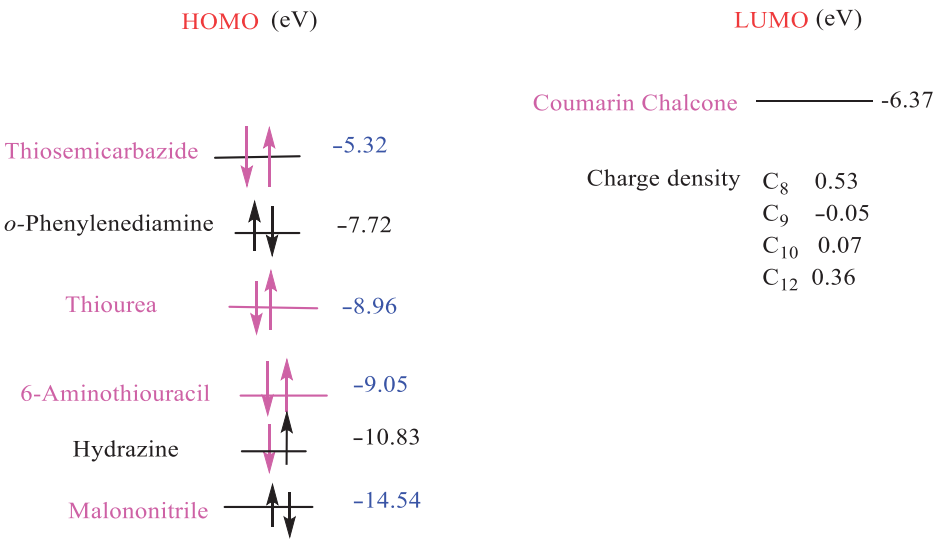

Figure 2. Outline the E_{HOMO} of nucleophiles toward E_{LUMO} of the starting material.

Table 1. Global reactivity indices and energy level distribution of frontier orbitals.

Compound	E_{HOMO}	E_{LUMO}	ΔE	I^a	A^b	μ^c	η^d	ω^e	ΔN^f	S^g	A_{molec} (nm^2)
Doxorubicin	−6.69	−2.41	4.28	6.88	3.62	5.28	0.66	31.09	0.56	1.98	243.621
3	−7.66	−6.14	1.52	7.09	5.38	7.29	0.76	35.60	0.028	1.34	232.246
4	−7.95	−5.70	2.25	8.08	5.93	16.39	1.13	21.56	0.046	0.88	364.594
5	−7.67	−4.40	3.27	7.36	4.36	6.62	1.63	13.366	0.0748	0.61	863.013
6	−7.80	−3.53	4.27	8.03	3.29	7.77	2.14	13.88	0.0720	0.46	761.829
7	−8.88	−2.67	6.21	8.69	2.78	6.13	3.16	102.6	0.023	0.39	232.246
8	−9.38	−4.53	4.85	9.65	4.85	7.03	2.51	62.02	0.017	0.398	265.246
9	−4.754	−3.604	1.15	4.96	3.82	4.23	0.60	5.36	0.126	1.67	609.594
10	−8.41	−2.96	5.45	7.36	4.36	5.86	2.83	48.59	0.095	0.349	493.013
11	−7.75	−4.98	2.77	7.66	4.66	4.04	1.39	12.94	0.077	0.719	687.625
12	−7.67	−4.56	3.11	7.63	4.24	−3.51	1.55	11.65	0.086	0.645	756.888
13	−7.46	−4.35	3.11	7.49	4.38	3.25	1.56	11.49	0.087	0.64	488.744
14	−5.40	−5.15	0.25	5.88	5.23	8.24	0.13	113.78	0.0087	7.69	377.146
15	−7.25	−4.67	2.58	7.26	4.66	5.14	1.29	10.24	0.09776	0.775	491.093
16	−6.88	−4.69	2.19	6.73	4.39	2.67	1.10	13.62	0.073	0.909	344.641
17	−7.51	−4.62	2.89	7.62	4.38	0.43	1.45	12.42	0.80	0.689	411.210

[a]Ionization potential, [b]Electron affinity, [c]Chemical potential, [d]Hardness, [e]Electrophilicity index, [f]nucleophilicity index, [g]Softness.

thermodynamically intermediate. This means in the case of malononitrile, it is a thermodynamic stable intermediate (cf. Figure 2).

So, DFT simulation helped us to know why the reactions of chalcone **3** with malononitrile, hydrazine hydrate, thiourea, thiosemicarbazide, and 6-aminothiouracil did not afford the expected heterocyclic compounds **4, 8, 11, 13,** and **16** and they yielded newly heterocyclic compounds **5, 9, 12, 14** and **17**, respectively. The structures have been supported by full spectral analysis and microanalytical data. Quantum chemical parameters calculation is using the density functional theory (DFT) method for the calculations of the newly synthesized compounds (Table 1). The high E_{HOMO} is likely to indicate a strong tendency of the molecule to donate electrons. The low values of the energy gap ($\Delta E = E_{LUMO} - E_{HOMO}$) will render good efficiencies.[30] The dipole moment,

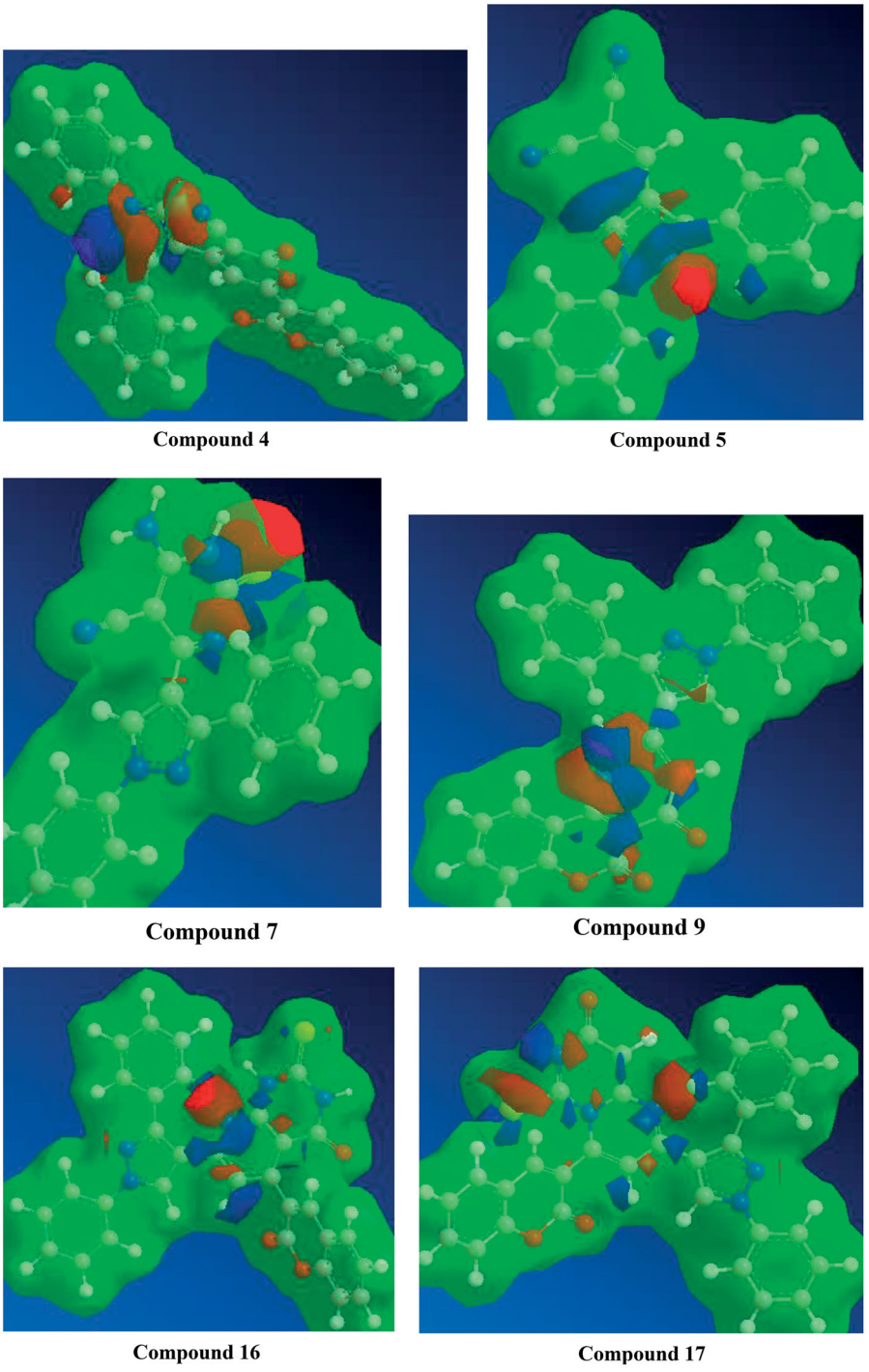

Figure 3. Outline the optimized structures **4–17** and the standard, doxorubicin (see more in the supplemental figures).

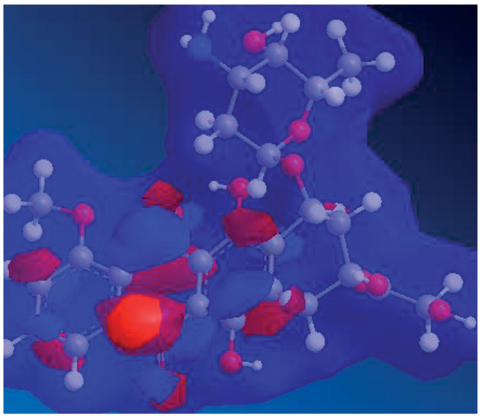

Doxorubicin

Figure 3. Continued.

Table 2. Outline the minimized energy and electron density of the tautomers of the more effective anticancer compounds **9** and **17**.

Compound no	$E_{Cal/mol}$	ΔE_{eV}	μ_{Dipole}	$e_{Charge\ density}$ diazepine N_{11}, N_{12}	E_{HOMO}	E_{LUMO}	$e_{Charge\ density}$ pyrimidine $N_{6\ bridge\ head}$
9a	78.70	1.21	15.55	0.246, 0.256	0.753	1.746	
9b	67.67	1.28	4.08	0.807, 0.434	−2.74	−4.02	
17a	69.5	2.89	0.43		−7.51	−4.62	0.468
17b	90.1	2.20	3.6		−7.0	−4.8	0.616
17c	102.0	6.6	6.6		−6.70	−4.50	0.587

hardness, softness, and surface area (nm^2) for newly pyrazole derivatives carrying hydrophobic groups were agreed with an excellent explanation for the synthesized compounds and their anticancer efficiency. Also, the Ionization potential (I, eV), transferred electrons, and charge density distribution (ΔN) indicate the greater value pyrazole derivatives **5, 9, 12, 14,** and **17** have the maximum transfer of electron and hence, greater tendency of adsorption and inhibition for the cancer cell. The optimization structures of the synthesized pyrazole **3–17** as outlined in Figure 3 (see more in the supplemental figures).

Quantum chemical parameters calculations using density functional theory (DFT) method used for the calculations of the synthesized compounds are in good agreement with the anticancer efficiency (Table 1). The listed results indicate that the values of gap energy (ΔE), where $\Delta E = E_{LUMO} - E_{HOMO}$, follow the order: heterocyclic derivatives **9 < 17 <** doxorubicin. Compounds having small ΔE values are generally referred to as soft compounds, that are more reactive toward radical surface interactions; being capable of donating electrons easily to hole surface.[31] The scavenging ability toward positive hole, tumor, radical, and oxygen removable not only depended upon E_{HOMO} values but also, the number of heteroatoms, electron distributions, surface area, and lipophilicity must be considered. The dipole moment, softness (ϭ, eV^{-1}), and surface area (nm^2)

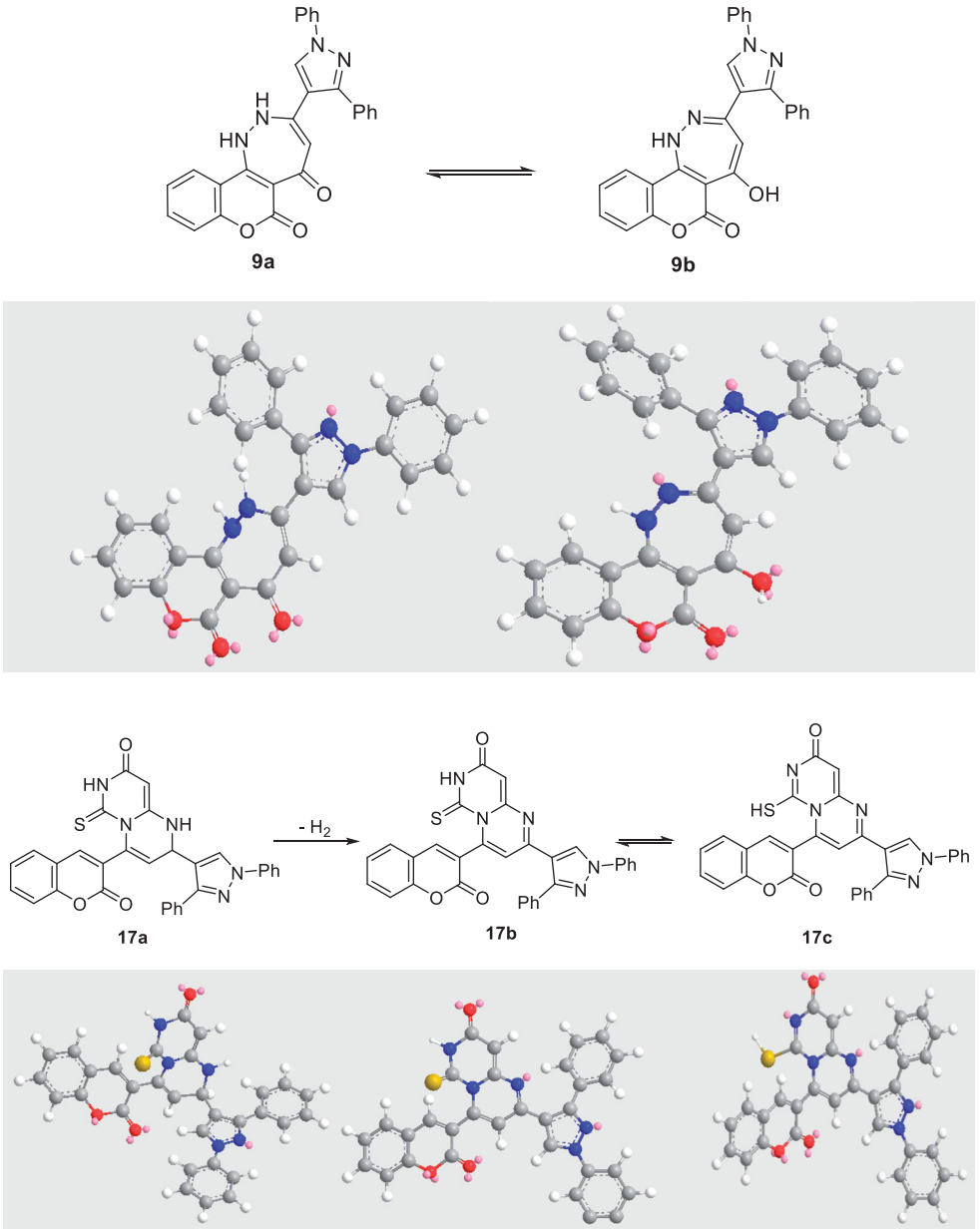

Figure 4. Structures of compounds **9** and **17**.

for most potent synthesized compounds carrying hydrophobic groups were agreed to an excellent correlation between oxidation inhibition efficiencies.

On the other hand, the minimized energy (kcal/mol), dipole moment, ionization potential (I, eV), transferred electrons, and charge density distribution (ΔN) revealed that the greater value of 0.126 and 0.8 for pyrazole **9** and **17**, respectively indicates the maximum transfer of electron and hence, greater tendency of scavenging radicals and rapidly reduce oxygen to superoxide ($O2^{\bullet-}$)[32] (see more in Table 2).

Table 3. Cytotoxic activity of some compounds against human tumors.

	In vitro cytotoxicity IC_{50} (μM)[a]	
Comp.	HePG-2	MCF-7
doxorubicin	4.50 ± 0.3	4.17 ± 0.2
3	68.96 ± 3.3	81.57 ± 4.1
6	36.50 ± 2.3	70.18 ± 3.6
9	12.68 ± 1.0	9.16 ± 0.7
10	56.24 ± 3.0	51.72 ± 2.8
12	43.07 ± 2.6	26.28 ± 1.9
14	59.12 ± 3.1	38.91 ± 2.2
15	30.61 ± 2.1	45.05 ± 2.5
17	19.32 ± 1.5	14.34 ± 1.2

[a]IC_{50} (μM): 1–10 (very strong), 11–20 (strong), 21–50 (moderate), 51–100 (weak), and above 100 (non-cytotoxic).

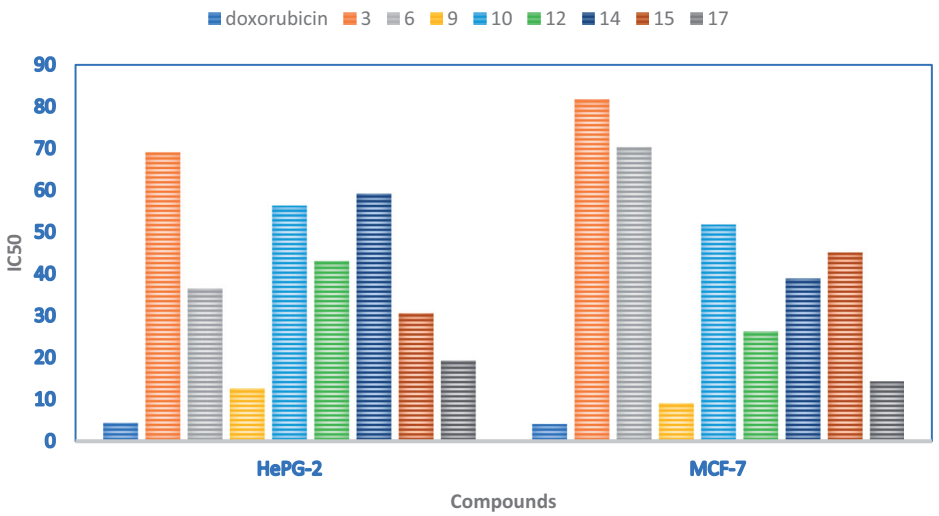

Figure 5. IC_{50} of the tested compounds.

Biological screening

It was shown that several enzymes including the cytochrome P450 reductase, NADH dehydrogenase, and xanthine oxidoreductase could reduce doxorubicin *via* a one-electron reduction mechanism giving rise to the phenate radical intermediate that can rapidly reduce oxygen to superoxide ($O_2^{\bullet-}$) *via* a futile redox-cycling mechanism.[33] In the presence of a redox-active metal ion such as iron (III), hydroxyl radicals are formed *via* the Fenton mechanism. Chelators such as desferrioxamine inhibit the formation of hydroxyl radicals through inhibition of the Haber-Weiss mechanism. Based on these *in vitro* studies, redox activation of newly synthesized compounds **9** and **17** to $O_2^{\bullet-}$, hydrogen peroxide (H_2O_2), and iron-catalyzed hydroxyl radical formation was suggested to be a similar mechanism of doxorubicin toxicity.[32] Oxidative stress is thought to be primarily responsible for phenolic diazepine **9**, pyrimidinethiol **17**, and doxorubicin cardiotoxicity because the myocardial tissues lack sufficient antioxidant mechanisms.[34]

Compounds **9** and **17** are the stronger anticancer than the other synthesized compounds which may be due to their presence in more tautomeric structures (Table 2; Figure 4).

Pharmacology

Antiproliferative screening

The antiproliferative screening of the synthesized compounds was measured against two cell lines namely, Hepatocellular carcinoma (HePG-2) and Mammary gland breast cancer (MCF-7) using MTT assay.[35,36] The results in Table 3 and Figure 5 disclosed that the most potent compounds against two cell lines were **9** and **17** as compared to doxorubicin. The compounds **6, 12,** and **15** were moderately potent against HePG-2 cell line. Moderate activity was shown against MCF-7 cell line by the compounds **12, 14,** and **15**. The rest of the compounds were of weak activity.

Conclusion

A novel series of fused and pyrazole-based heterocyclic systems like chromenopyran, chromenodiazepine, diazepine, chromenopyrimidine, triazepinethione, benzodiazepine, and pyrimidopyrimidine derivatives, was prepared from the chalcone namely, 3-(3-(1,3-diphenyl-1*H*-pyrazol-4-yl)acryloyl)-2*H*-chromen-2-one. The antiproliferative activity screening of the synthesized compounds disclosed that the chromenodiazepine and pyrimidopyrimidine derivatives were the most potent against the two tumor cells namely, HePG-2 and MCF-7. DFT based on quantum chemical computation outline the structure optimization of the intermediate that reacted to afford the desired product.

Experimental

General

All melting points were measured on a GALLENKAMP electric melting point apparatus and are uncorrected. Chemicals and solvents used were obtained from commercial sources and used as received or dried by standard procedures. IR spectra (ν, cm^{-1}) were recorded using potassium bromide disks on Fourier Transform Infrared Thermo Electron Nicolet iS10 Spectrometer (Thermo Fisher Scientific Inc., Waltham, MA, USA) at Faculty of Science, Ain Shams University. The ^1H NMR spectra (δ_H, ppm) were recorded at 300 MHz on a Varian GEMINI (GEMINI, Manufacturing & Engineering Inc., Anaheim, CA, USA) utilizing tetramethyl silane (TMS) as an internal standard in deuterated dimethyl sulfoxide (DMSO-d_6) at Faculty of Science, Cairo University. The mass spectra (MS) were recorded on Shimadzu GC-MS-QP-1000 EX mass spectrometer (Shimadzu Scientific Instruments, Inc., USA) operating at 70 eV at the Regional Center for Mycology and Biotechnology (RCMB) of Al-Azhar University, Cairo, Egypt. The reactions were monitored by thin-layer chromatography (TLC) using Merck Kiesel gel 60 F_{254} analytical sheets obtained from Fluka, Switzerland. The antiproliferative activity was carried out at the Faculty of Pharmacy, Mansoura University, Mansoura, Egypt.

The starting pyrazole-4-carbaldehyde derivative **2** was previously prepared.[27]

3-(3-(1,3-Diphenyl-1H-pyrazol-4-yl)acryloyl)-2H-chromen-2-one (3)

A mixture of 3-acetylcoumarin **1** (0.05 mol) and pyrazole aldehyde **2** (0.05 mol) in absolute ethanol (20 mL) including piperidine (0.1 mL) was refluxed for 2 h. The solid obtained while hot was filtered off and recrystallized from *n*-butanol to furnish chalcone **3** as yellow crystals, mp. 260–262 °C, yield 90%. IR: 1722 (C=O coumarin), 1655 (C=O ketone). ^{1}H NMR (300 *MHz*, DMSO-d_6): 9.29 (s, 1H, C5-H pyrazole), 8.65 (s, 1H, C4-H coumarin), 8.00–7.40 (m, 16H, Ar-H). MS, *m/z* (%): 418 ($M^{+\cdot}$, 22), 341 (4), 268 (9), 245 (89), 173 (25), 115 (26), 77 (100). Anal. Calcd. for $C_{27}H_{18}N_2O_3$ (418.45): C, 77.50; H, 4.34; N, 6.69. found: C, 77.32; H, 4.27; N, 6.71%.

2-Amino-4-(1,3-diphenyl-1H-pyrazol-4-yl)-5-oxo-4H,5H-pyrano[3,2-c]chromene-3-carbonitrile (6)

A mixture of arylidine malononitrile **5** (0.01 mol) and 4-hydroxycoumarin (0.01 mol) in absolute ethanol (20 mL) including triethylamine (0.1 mL) was refluxed for 10 h (TLC), the contents were poured onto ice-cold water and then acidified by dil. HCl (10%). The deposited solid was filtered off and gray crystals were obtained after crystallization from ethanol, mp. 228–230 °C, yield 57%. IR: 3392, 3318 (NH_2), 2193 (C≡N), 1710 (C=O coumarin). ^{1}H NMR (300 *MHz*, DMSO-d_6): 8.58 (s, 1H, C5-H pyrazole), 7.87–7.29 (m, 14H, Ar-H), 7.26 (br.s, 2H, NH_2, exchangeable), 4.70 (s, 1H, C4-H pyran). MS, *m/z* (%): 458 ($M^{+\cdot}$, 22), 419 (8), 393 (59), 392 (100), 315 (19), 270 (30), 243 (21), 120 (14), 92 (41), 77 (55). Anal. Calcd. for $C_{28}H_{18}N_4O_3$ (458.48): C, 73.35; H, 3.96; N, 12.22. found: C, 73.22; H, 3.89; N, 12.25%.

Full experimental details, tables, figures, spectroscopic data can be found in supplemental files.

Disclosure statement

No potential conflict of interest was reported by the author(s).

ORCID

Sayed K. Ramadan http://orcid.org/0000-0003-2743-6544
Sameh A. Rizk http://orcid.org/0000-0002-8232-5399

References

[1] Orlikova, B.; Tasdemir, D.; Golais, F.; Dicato, M.; Diederich, M. *Genes Nutr.* **2011**, *6*, 125–147. DOI: 10.1007/s12263-011-0210-5.
[2] Kenchappa, R.; Bodke, Y. D.; Chandrashekar, A.; Sindhe, M. A.; Peethambar, S. K. *Arabian J. Chem.* **2017**, *10*, S3895–S3906. DOI: 10.1016/j.arabjc.2014.05.029.
[3] Singh, A. D.; Kumar, A.; Saini, S.; Prabha, H. *APJHS* **2017**, *4*, 84–93. DOI: 10.21276/apjhs.2017.4.4.21.
[4] Anees Rahman, K. N.; Haribabu, J.; Balachandran, C.; Bhuvanesh, N. S. P.; Ramasamy Karvembu, R.; Sreekanth, A. *Polyhedron.* **2017**, *135*, 26–35. DOI: 10.1016/j.poly.2017.06.044.

[5] (a) Abdou, M. M. *Arabian J. Chem.*. **2017**, *10*, S3664–S3675. DOI: 10.1016/j.arabjc.2014.04.005.(b) Gomha, S. M.; Zaki, Y. H.; Abdelhamid, A. O. *Molecules*. **2015**, *20*, 21826–21839. DOI: 10.3390/molecules201219803.

[6] (a) Peng, X. M.; Damu, G. L.; Zhou, C. H. *CPD*. **2013**, *19*, 3884–3930. DOI: 10.2174/1381612811319210013.(b) Salem, M. A. I.; Marzouk, M. I.; El-Kazak, A. M. *Molecules*. **2016**, *21*, 249 DOI: 10.3390/molecules21020249.

[7] (a) Halim, K. N. M.; Ramadan, S. K.; Rizk, S. A.; El-Hashash, M. A. *Synth. Commun*. **2020**, *50*, 1159–1175. DOI: 10.1080/00397911.2020.1720739. (b) Ramadan, S. K.; Halim, K. N. M.; Rizk, S. A.; El-Hashash, M. A. *J. Iran. Chem. Soc*. **2020**, *17*, 1575–1589. DOI: 10.1007/s13738-020-01880-8.(c) Halim, K. N. M.; Rizk, S. A.; El-Hashash, M. A.; Ramadan, S. K. *J. Heterocyclic Chem*. **2021**, *58*, 636–645. DOI: 10.1002/jhet.4204.

[8] (a) Ramadan, S. K.; Abou-Elmagd, W. S. I. *Synth. Commun*. **2018**, *48*, 2409–2419. DOI: 10.1080/00397911.2018.1491995. (b) El-Helw, E. A. E.; Gado, M. M.; El-Ziaty, A. K. *J. Iran. Chem. Soc*. **2020**, *17*, 1479–1492. DOI: 10.1007/s13738-020-01873-7.(c) Ramadan, S. K.; El-Ziaty, A. K.; Ali, R. S. *J. Heterocyclic Chem*. **2021**, *58*, 290–304. DOI: 10.1002/jhet.4168.

[9] Tao, X. X.; Duan, Y. T.; Chen, L. W.; Tang, D. J.; Yang, M. R.; Wang, P. F.; Xu, C.; Zhu, H. L. *Bioorg. Med. Chem. Lett*. **2016**, *26*, 677–683. DOI: 10.1016/j.bmcl.2015.11.040.

[10] Kamal, A.; Shaik, A. B.; Jain, N.; Kishor, C.; Nagabhushana, A.; Supriya, B.; Kumar, G. B.; Chourasiya, S. S.; Suresh, Y.; Mishra, R. K.; Addlagatta, A. *Eur. J. Med. Chem*. **2015**, *92*, 501–513. DOI: 10.1016/j.ejmech.2013.10.077.

[11] Yao, Y.; Liao, C.; Li, Z.; Wang, Z.; Sun, Q.; Liu, C.; Yang, Y.; Tu, Z.; Jiang, S. *Eur. J. Med. Chem*. **2014**, *86*, 639–652. DOI: 10.1016/j.ejmech.2014.09.024.

[12] El-Helw, E. A. E.; El-Badawy, A. A. *J. Heterocycl. Chem*. **2020**, *57*, 2354. DOI: 10.1002/jhet.3948.

[13] Ramadan, S. K.; El-Helw, E. A. E.; Sallam, H. A. *Heterocycl. Commun*. **2019**, *25*, 107–115. DOI: 10.1515/hc-2019-0008.

[14] Ramadan, S. K.; Sallam, H. A. *J. Heterocyclic Chem*. **2018**, *55*, 1942–1954. DOI: 10.1002/jhet.3232.

[15] (a) Abou-Elmagd, W. S. I.; El-Ziaty, A. K.; Elzahar, M. I.; Ramadan, S. K.; Hashem, A. I. *Synth. Commun*. **2016**, *46*, 1197–1208. DOI: 10.1080/00397911.2016.1193755. (b) Ramadan, S. K.; Shaban, S. S.; Hashem, A. I. *Synth. Commun*. **2020**, *50*, 185–196. DOI: 10.1080/00397911.2019.1691737.

[16] Goudgaon, N. M.; Sheshikant, B. U.; Dhage, D. *Heterolett*. **2012**, *2*, 154.

[17] Powers, D. G.; Casebier, D. S.; Fokas, D.; Ryan, W. J.; Troth, J. R.; Coffen, D. L. *Tetrahedron*. **1998**, *54*, 4085–4096. DOI: 10.1016/S0040-4020(98)00137-9.

[18] Rizk, S. A.; El-Hashash, M. A.; Mostafa, K. K. *Egypt*. J. Chem. **2008**, *51*, 116.

[19] Rizk, S. A.; Elsayed, G.; El-Hashash, M. A. *J. Iran. Chem. Soc*. **2018**, *15*, 2093–2105. DOI: 10.1007/s13738-018-1402-3.

[20] El-Hashash, M. A.; Rizk, S. A.; El-Bassiouny, F. A.; Guirguis, D. B.; Khairy S. M., Guirguis , *Egypt J. Chem*. **2017**, *60*, 407.

[21] El-Hashash, M. A.; Darwish, K. M.; Rizk, S. A.; El-Bassiouny, F. A. *Pharmaceuticals*. **2011**, *4*, 1032–1051. DOI: 10.1155/2011/295491.

[22] Youssef, A. M.; El-Ziaty, A. K.; Abou-Elmagd, W. S. I.; Ramadan, S. K. *J. Heterocyclic Chem*. **2015**, *52*, 278–283. DOI: 10.1002/jhet.1943.

[23] Morsy, A. R. I.; Ramadan, S. K.; Elsafty, M. M. *Med. Chem. Res*. **2020**, *29*, 979–988. DOI: 10.1007/s00044-020-02538-z.

[24] Ramadan, S. K.; Elrazaz, E. Z.; Abouzid, K. A. M.; El-Naggar, A. M. *RSC Adv*. **2020**, *10*, 29475–29492. DOI: 10.1039/D0RA05943A.

[25] El-Naggar, A. M.; Ramadan, S. K. *Synth. Commun*. **2020**, *50*, 2188–2198. DOI: 10.1080/00397911.2020.1769673.

[26] (a) Ramadan, S. K.; Hashem, A. I.; Abou-Elmagd, W. S. I.; El-Ziaty, A. K. *J. Heterocycl. Chem*. **2017**, *54*, 3711.(b) Ramadan, S. K.; El-Helw, E. A. E. *J. Chem. Res*. **2018**, *42*, 332–336. DOI: 10.3184/174751918X15295796734379.

[27] Rathelot, P.; Azas, N.; El-Kashef, H.; Delmas, F.; Giorgio, C. D.; Timon-David, P.; Maldonado, J.; Vanelle, P. *Eur. J. Med. Chem*. **2002**, *37*, 671–679. DOI: 10.1016/s0223-5234(02)01388-0.
[28] Li, J.-P.; Qiu, J.-K.; Li, H.-J.; Zhang, G.-S. *J. Chin. Chem. Soc*. **2011**, *58*, 268–271. DOI: 10.1002/jccs.201190087.
[29] El-Taib Heakal, F.; Rizk, S. A.; Elkholy, A. E. *J. Mol. Struct*. **2018**, *328*, 1152.
[30] Chirlian, L. E.; Francl, M. M. *J. Comput. Chem*. **1987**, *8*, 894–905. DOI: 10.1002/jcc.540080616.
[31] Elkholy, A. E.; Rizk, S. A.; Rashad, A. M. *J. Mol. Struct*. **2019**, *788*, 1175.
[32] Dhingra, R.; Margulets, V.; Chowdhury, S. R.; Thliveris, J.; Jassal, D.; Fernyhough, P.; Dorn, G. W.; Kirshenbaum, L. A. *Proc. Natl. Acad. Sci. USA*. **2014**, *111*, E5537–E5544. DOI: 10.1073/pnas.1414665111.
[33] Kalyanaraman, B. *Redox Biol*. **2020**, *29*, 101394. DOI: 10.1016/j.redox.2019.101394.
[34] Fang, X.; Wang, H.; Han, D.; Xie, E.; Yang, X.; Wei, J.; Gu, S.; Gao, F.; Zhu, N.; Yin, X.; et al. *Proc. Natl. Acad. Sci. USA*. **2019**, *116*, 2672–2680. DOI: 10.1073/pnas.1821022116.
[35] Mosmann, T. *J. Immunol. Methods*. **1983**, *65*, 55–63. DOI: 10.1016/0022-1759(83)90303-4.
[36] Denizot, F.; Lang, R. *J. Immunol. Methods*. **1986**, *22*, 271.